

---

# Simple improved control of phase error compensation for low power operation of PV grid-connected inverter with LCL filter

**Baochao C. Wang, Manuela Sechilariu, Fabrice Locment**

*AVENUES-GSU, Université de Technologie de Compiègne  
Rue du Docteur Schweitzer, 60200 Compiègne, France*

*fabrice.locment@utc.fr*

---

*ABSTRACT. Obvious grid power factor degradation can often be observed when using LCL filter for grid-connected photovoltaic systems. This paper analyzes degradation causes and a phase error compensation structure is proposed. Experimental results conclude that the proposed compensation structure improves the grid power quality in case of low PV production, in both power factor and harmonics.*

*RÉSUMÉ. Une dégradation évidente du facteur de puissance du réseau électrique peut souvent être observée lors de l'utilisation d'un filtre LCL pour les systèmes photovoltaïques. Cet article analyse la cause de la dégradation et une structure de compensation d'erreur de phase est proposée. Les résultats expérimentaux montrent que la structure de compensation proposée améliore les performances de la qualité du réseau en cas de faible production photovoltaïque, tant pour le facteur de puissance que pour les harmoniques.*

*KEYWORDS: PV grid-connected inverter, LCL filter, control, phase error compensation.*

*MOTS-CLÉS : onduleur PV connecté au réseau, filtre LCL, contrôle, compensation d'erreur de phase.*

---

DOI:10.3166/EJEE.17.27-45 © 2014 Lavoisier

## 1. Introduction

Photovoltaic (PV) sources and wind turbine play an important role in distributed generation. Nevertheless, these renewable distributed powers undergo strong variation over time and can hardly be precisely predicted. Hence, a filter to satisfy high power quality over the full power operation range is required. The filter should enhance the important role of grid-connected inverter, in distributed generation, by two sides. Firstly, the grid-side current has to be controlled to follow given current reference to provide the active power and reactive power demand with as less distortion as possible. Secondly, with the power electronic devices working in PWM mode, the inverter output, voltage and current, includes switching noise and harmonics. The filter should be able to reduce frequency noise, generated by the PWM inverter, and harmonics.

Traditionally, as L filter, a serial inductor is used, which is simple to control and can offer precisely current phase and amplitude control over the full operating range. However, as the attenuation ability is not satisfying for the full power range, a larger value inductance is required to get smooth enough the current. But, the increasing inductance value is not cost-effective and could also reduce the dynamic performance of the system.

LCL filter could be one of the solutions. Compared with the L filter, LCL filter could provide three times attenuation ability for high frequencies with less component values. Regarding PV generators, due to the strong variation of solar irradiation for a relatively short period of time, the grid injected power is usually strongly varying with large differences. In case of high solar irradiation, corresponding to high level power injection, the LCL performance is satisfactory. While in case of weak solar irradiation, the injected power could have a very low level and, for low power operation, the LCL filter control usually results in obvious power factor degradation. Moreover, by different feedback methods of LCL filter control, the grid voltage could be a source which introduces more distortions in the grid current: phase error, amplitude error and harmonics. Thus, the low power operation of PV grid-connected inverter needs to be improved in order to inject power with high quality power injection.

According to recent researches (cf. Dannehl *et al.*, 2009; Fei *et al.*, 2009; Figueres *et al.*, 2009; Gabe *et al.*, 2009; Jalili *et al.*, 2009; Mariethoz *et al.*, 2009; Dannehl *et al.*, 2010, 2010; Guoqiao *et al.*, 2010; Hea-Gwang *et al.*, 2010; Agorreta *et al.*, 2011; Dannehl *et al.*, 2011; Mohamed, 2011), the LCL filter current control strategies are based on grid current feedback (cf. Dannehl *et al.*, 2009; Fei *et al.*, 2009; Mariethoz *et al.*, 2009; Dannehl *et al.*, 2011; Mohamed, 2011) and inverter current feedback (cf. Dannehl *et al.*, 2009; Figueres *et al.*, 2009; Gabe *et al.*, 2009; Jalili *et al.*, 2009; Dannehl *et al.*, 2010; Dannehl *et al.*, 2010; Hea-Gwang *et al.*, 2010; Agorreta *et al.*, 2011; Dannehl *et al.*, 2011). In Guoqiao *et al.* (2010), the currents are both used with corresponding weight to form a combined feedback. Grid current feedback control usually involves more control bandwidth and is

tended to be unstable; the control loop gain is insufficient due to stability limit. Inverter current feedback requires less control bandwidth and offers sufficient control loop gain. It is more stable and robust and so is more often studied in the literature. However, the inverter current feedback cannot totally reject grid voltage disturbance in the grid current output.

In grid current feedback, extra feedback, or inner control loop which can increase the robustness of the control strategy, are often reported in literature (cf Fei *et al.*, 2009; Mariethoz *et al.*, 2009; Mohamed, 2011). Capacitor current inner loop feedback has the advantage of add damping to resonance; however, due to insufficient gain of current control, it is difficult to track low power command as mentioned by Fei *et al.* (2009).

Regarding different controllers used, we note that they have different influence on grid current distortion. PI controller, relatively simple and robust, is the most widely used (cf. Dannehl *et al.*, 2009; Fei *et al.*, 2009; Figueres *et al.*, 2009; Jalili *et al.*, 2009; Hea-Gwang *et al.*, 2010; Agorreta *et al.*, 2011; Dannehl *et al.*, 2011). In frequency domain, it provides continuous gain. PI controller combined with state space control is studied by Dannehl *et al.* (2010). It makes state space control parameter tuning more simplified. Based on the fact that, in grid-connected inverter control, the current reference and grid voltage contain some frequency elements, Proportional-Resonant (PR) controller works on the principle of providing relatively significant controller gain at specified frequencies (Gabe *et al.*, 2009; Guoqiao *et al.*, 2010). Usually the major odd-order harmonics are considered. Compared with PI controller, PR controller provides more significant gain at desired frequency and less gain at natural resonance frequency introduced by LCL filter; so, the natural resonance can be eased. However, PR controller is prone to numerical problems.

Model predictive control, pole placement and state space control are used (Mariethoz *et al.*, 2009; Dannehl *et al.*, 2010; Mohamed, 2011). These methods are usually depending on extra sensor or precise model parameter, or control parameter tuning procedures. Thus, the robustness could be an issue.

In order to deal with resonance problems, different damping strategies are used: passive damping (cf. Figueres *et al.*, 2009; Guoqiao *et al.*, 2010) that is simple, robust and does not need additional sensors, active damping with multi-loop control (cf. Fei *et al.*, 2009; Agorreta *et al.*, 2011), capacitor voltage lead-lag feedback (cf. Jalili *et al.*, 2009; Dannehl *et al.*, 2010), filter based damping (cf. Dannehl *et al.*, 2009; Dannehl *et al.*, 2011) and modern control strategy (cf. Mariethoz *et al.*, 2009; Dannehl *et al.*, 2010; Mohamed, 2011). Active damping either involves additional sensors or complex computation. Filter based active damping does not need additional sensors, but could decrease the system dynamic performances.

With inverter current feedback and PI or PR controller without compensation, the grid voltage cannot be rejected in grid current output and causes grid current phase error. The case is more obvious in low power operation and high grid voltage.

For grid current feedback combined with capacitor current inner loop, Xuehua *et al.* (2010) propose a feed-forward compensation involving proportional, derivative and second derivative of grid voltage to deal with current distortion due to insufficient control loop gain. For inverter current feedback, the grid voltage introduces reactive power and harmonics in the grid current. Grid voltage feed-forward for compensating the grid voltage is used (cf. Abeyasekera *et al.*, 2005; Harnefors *et al.*, 2008; Xuehua *et al.*, 2010), but direct grid voltage feed-forward does not solve the problem. Grid voltage related distortion is analyzed by Abeyasekera *et al.* (2005), and compensation using capacitor current is proposed, while Sung Yeul *et al.* (2008) proposed compensation structure using capacitor voltage. Capacitor current and capacitor voltage compensation are approximations of grid voltage compensation, and involve additional sensor for compensation. In this paper, by selecting inverter current feedback, the same compensation concept is employed, but the grid voltage is directly used for compensation with properly selecting sampling point, which do not need additional sensor.

This paper is structured as follows: section 2 introduces overview of the PV grid-connected inverter by LCL filter and hardware configurations. Section 3 analyzes phase error cause in different current feedback strategies using transfer function, and selects inverter current feedback as control strategy. Section 4 proposes a simplified compensation using grid voltage. Section 5 combines PLL and passive damping with the simplified compensation. PLL generates smooth fundamental grid voltage to avoid EMI problem in measurement. Passive damping further simplifies the compensation structure from differential form to proportional form, as well as improves the power quality with reasonable cost. By experimental results in section 6, it is concluded that the proposed compensation structure improves the power factor and reduces current distortion in low power operation.

## 2. System description

The PV grid-connected inverter and LCL filter are shown in Figure 1, where  $L_{PV}$ ,  $C_{DC}$ ,  $L_I$ ,  $L_G$ ,  $C$  and  $R$  are PV inductor, DC bus capacitor, inverter-side inductor, grid-side inductor, filter capacitor and damping resistor;  $u_{PV}$ ,  $i_{PV}$ ,  $u_{DC}$ ,  $u_I$ ,  $u_C$  and  $u_G$  are PV array (PVA) voltage, PVA current, DC bus voltage, inverter output voltage, capacitor branch voltage and grid voltage. The resistor  $R$  provides damping of resonance effects, otherwise, for  $R = 0$ , the filter is without passive damping. The system inverter consists in three-leg power, one ( $A_1$ ) for extracting maximum power from PVA, and a single phase H-bridge ( $A_2, A_3$ ) for injecting power into the grid. Power system parameters are listed in Table 1.

Concerning the PVA, it contains 16 panels (Solar-Fabrik SF-130/2-125 with the open circuit voltage 21.53V, maximum power point voltage 17.50V and maximum power point current 7.14A at standard conditions 1000W/m<sup>2</sup>, 25°C). In order to

produce maximum power, the PVA is operated with P&O algorithm, as described by Houssamo *et al.* (2010).

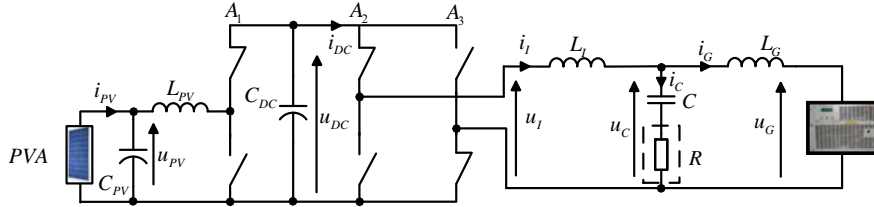


Figure 1. PV grid-connected inverter by LCL filter

Table 1 System parameters

Symbol	Description	Value
$u_{DC}$	DC bus voltage	400V
$u_G$	grid voltage	230V
$f_G$	grid voltage frequency	50Hz
$L_I$	inverter-side inductance	20mH
$C$	capacitor	10 $\mu$ F
$R$	damping resistor	0 $\Omega$ /16 $\Omega$
$L_G$	grid-side inductance	5mH
$f_c$	control frequency	10kHz

The inductors  $L_I$  and  $L_G$  have inherent internal resistance that is neglected in this study, considering that the internal resistance is relatively small compared to the impedance provided by the inductance. Hence, the block diagram of the system is shown in Figure 2.

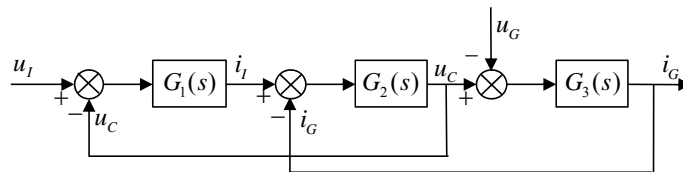


Figure 2. Block diagram of LCL filter

In Figure 2, the concerned transfer function in  $s$  domain is  $G_1 = \frac{1}{L_I s}$ ,  $G_2 = \frac{1}{Cs} + R$ ,  $G_3 = \frac{1}{L_G s}$ , where  $s$  is the Laplace operator. Each of these three transfer functions offers infinite gain for DC and decreases of -20dB/Dec at high frequencies.

Grid current  $i_G$  is affected by two elements: the inverter voltage  $u_I$  and the grid voltage  $u_G$ . In a classical control problem,  $u_G$  is normally considered as disturbance for the control. It is supposed that a controller with enough gain at the same frequency of disturbance could reject this disturbance in the output, and only the transfer function concerning  $u_I$  and  $i_G$  are considered for the controller design. However, according to the feedback structure, as analyzed in section 3, this is not always valid. Taking into consideration both voltages,  $u_I$  and  $u_G$ , the closed loop relationship is given in (1) :

$$i_G(s) = \frac{G_1 G_2 G_3}{1 + G_1 G_2 + G_2 G_3} u_I(s) - \frac{(1 + G_1 G_2) G_3}{1 + G_1 G_2 + G_2 G_3} u_G(s) \quad (1)$$

The system is a third order system. According to different feedback and control structures, the closed loop relationship of  $i_G$ ,  $u_I$  and  $u_G$  varies.

### 3. Current feedback selection and grid voltage influence

In this section, aiming the stability and phase error cause, two current control strategies are analyzed: feedback of the inverter-side current and the grid-side current. Stability and phase error principle are demonstrated using transfer function.

#### 3.1. Grid-side current feedback

The grid-side current feedback control block diagram is shown in Figure 3.

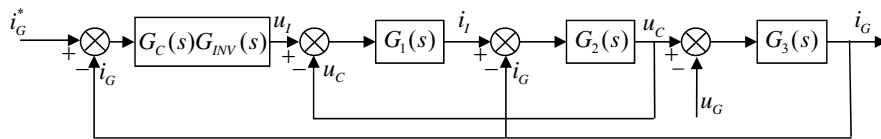


Figure 3. Current control by grid-side current feedback

$G_C$  is the controller transfer function and  $G_{INV}$  is the inverter transfer function describing the output. Neglecting switching transient in one PWM period, as the

controller duty cycle output range  $-1\sim 1$  represents the inverter output voltage range  $-u_{DC}\sim u_{DC}$ ,  $G_{INV}(s)$  can be considered as a gain  $u_{DC}$ . The open loop transfer function is given as:

$$\frac{i_G(s)}{i_G^*(s)} = \frac{G_c G_{INV} G_1 G_2 G_3}{1 + G_1 G_2 + G_2 G_3} \quad (2)$$

The closed loop relationship is:

$$i_G(s) = \frac{G_1 G_2 G_3 G_c G_{INV}}{1 + G_1 G_2 + G_2 G_3 + G_1 G_2 G_3 G_c G_{INV}} i_G^*(s) - \frac{G_3 + G_1 G_2 G_3}{1 + G_1 G_2 + G_2 G_3 + G_1 G_2 G_3 G_c G_{INV}} u_G(s) \quad (3)$$

with  $i_G^*$  the grid current reference.

Supposing the controller could offer large enough gain at the frequency domain of grid current reference  $i_G^*$  and  $u_G$ , in (3) all the product elements, in both denominator and nominator, that are not containing  $G_c$  can be neglected. Thus, (3) can be simplified as:

$$i_G(s) = i_G^*(s) \quad (4)$$

Following (4), with controller able providing sufficient gain, the grid current could follow the grid current reference, and  $u_G$  influence can be totally rejected, which is an ideal case. In real application, the stability problem could limit the controller gain, which could not be large enough for the necessary derivation from (3) to (4). The open loop Bode diagram of (2) is shown in Figure 4a, which gives the stability margin of grid current feedback control without damping. It is indicated at the top of the figure that phase margin (Pm in the figure) and gain margin (Gm in the figure) are negative, signifying that the control structure is unstable. Based on stability analyze, the system is more stable if it has larger positive margin in the open loop Bode diagram.

By Dannehl *et al.* (2009) the authors concluded that the grid current feedback control could be stable without passive damping, but only as long as the resonance frequency is between a quarter and half of the control frequency. However, the current distortion is still an issue. So, stability and power quality should be improved. By adding series damping resistor with the capacitor, the stability could be improved, and the open loop Bode diagram is shown in Figure 4b. It can be see the phase margin and gain margin are positive but relatively small, signifying the control loop gain could be limited for this control structure.

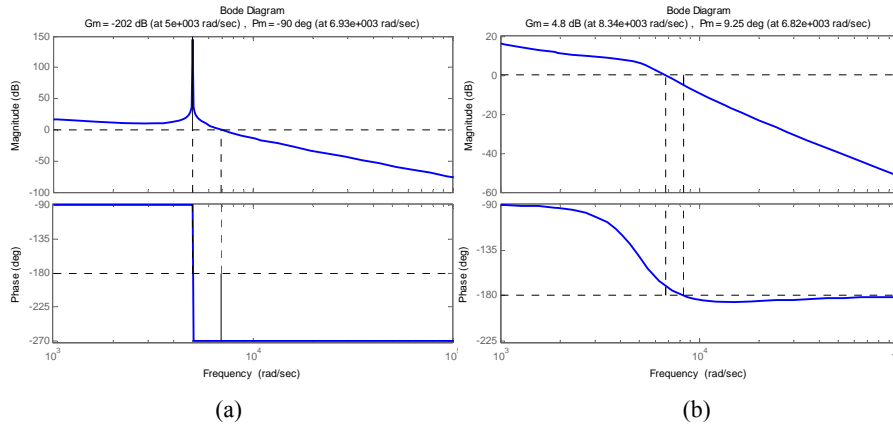


Figure 4. Stability margin of grid-side current feedback: (a) without damping resistor, (b) with damping resistor

With gain increasing, the stability margin decreases. The system could be stable only with small gain values. In fact, with the stability limit, the stable control loop gain could hardly satisfy the current control objective in low power operation. So, for grid current feedback, inner loop control, additional sensors and control with large bandwidth are required to improve the problem. However, in steady state of low power operation, the insufficient gain could give error to follow the current reference. Thus, other control structures are required.

### 3.2. Inverter-side current feedback

If the inverter current control is selected, the control block diagram is as in Figure 5. It is expected that the grid current  $i_G$  could follow the inverter current reference  $i_l^*$ .

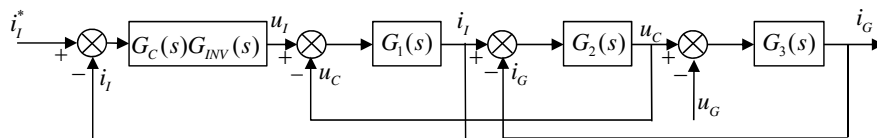


Figure 5. Current control by inverter-side current feedback

The stability is analyzed by open loop transfer function, which is shown in (5).

$$\frac{i_l}{i_l^*} = \frac{G_C G_{INV} G_1 (1 + G_2 G_3)}{1 + G_1 G_2 + G_2 G_3} \quad (5)$$

The stability margin of inverter current feedback control of (5) is shown in Figure 6. It can be seen for both cases of inverter current feedback, namely with or without passive damping, the system gain margin is infinite, meaning that the control is theoretically stable even with infinite control loop gain. The closed loop relationship of current feedback is shown in (6):

$$i_G(s) = \frac{G_C G_{INV} G_1 G_2 G_3}{1 + G_1 G_2 + G_2 G_3 + G_1 G_C G_{INV} + G_1 G_2 G_3 G_C G_{INV}} i_l^*(s) - \frac{G_3 (1 + G_1 G_2 + G_1 G_C G_{INV})}{1 + G_1 G_2 + G_2 G_3 + G_1 G_C G_{INV} + G_1 G_2 G_3 G_C G_{INV}} u_G(s) \quad (6)$$

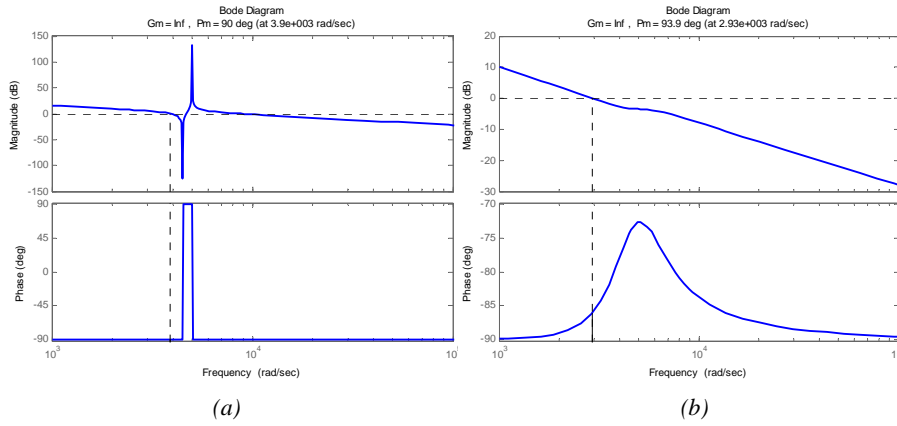


Figure 6. Stability margin of inverter-side current feedback: (a) without damping resistor, (b) with damping resistor

Supposing the controller could offer large enough gain (theoretically an infinite gain still maintains the stability of the control structure, while in practice the control loop gain cannot be infinite but still can be considered large enough), at the frequency domain of grid current reference  $i_G^*$  and  $u_G$ , in (6) all the product elements, in both denominator and nominator, that are not containing  $G_C$  can be neglected. Thus, (6) can be simplified as:

$$i_G(s) = \frac{G_2 G_3}{1 + G_2 G_3} i_l^*(s) - \frac{G_3}{1 + G_2 G_3} u_G(s) \quad (7)$$

From (7), it can be seen that only by controller parameter tuning design, even with ideal controller, the grid voltage  $u_G$  influence on  $i_G$  could not be totally rejected. When  $i_l^*$  decreases, the current control becomes worse and  $u_G$  influence becomes more obvious. The grid voltage influence affects not only current control amplitude, but also current phase and power factor. In addition, if the grid voltage includes harmonic distortion, the grid current also suffers the same frequency harmonics distortion.

For inverter-side current feedback, the control structure is stable and can operate with sufficient gain to follow the current reference. The inconvenience is that grid voltage introduces an output in the grid current, which normally is reactive power and causes obvious phase error and low power factor in low power operation.

For a low power operation, the two objectives are to follow the current reference and to reject the disturbance caused by the grid voltage. Using grid-side current feedback, the drawback is that the current could not follow the current reference in low power operation, because of insufficient controller gain limited by stability. While the inverter-side current feedback control has no problem of following current reference, disturbance rejection needs to be considered. Hence, making the choice of the inverter-side current control, the phase error elimination needs to be studied.

#### 4. Phase error compensation

The grid voltage related grid current distortion can be compensated by modifying the inverter-side current control reference as follow:

$$i_l^*(s) = i_G^*(s) + \frac{1 + G_1 G_2 + G_1 G_C G_{INV}}{G_C G_{INV} G_1 G_2} u_G(s) = i_G^*(s) + G_{COMP\_FULL} u_G(s) \quad (8)$$

By introducing (8) into (6) and supposing that the controller offers sufficient gain, which can be theoretically infinite, the grid voltage can be rejected from the grid current output as expressed by (9):

$$i_G(s) = \frac{G_C G_{INV} G_1 G_2 G_3}{1 + G_1 G_2 + G_2 G_3 + G_1 G_C G_{INV} + G_1 G_2 G_3 G_C G_{INV}} i_G^*(s) \approx i_G^*(s) \quad (9)$$

Thus, the full compensation transfer function is:

$$G_{COMP\_FULL} = \frac{1 + G_1 G_2 + G_1 G_C G_{INV}}{G_C G_{INV} G_1 G_2} \quad (10)$$

Due to discrete effect and control delay, the controller gain cannot reach infinite value, but can be still considered large enough. By ignoring the elements not containing  $G_C G_{INV}$  the compensation transfer function can be simplified as (11).

$$G_{COMP\_SIMP} = \frac{1}{G_2} = sC \quad (11)$$

Figure 7 shows Bode diagram of the compensation transfer function by full compensation and simplified compensation. It can be seen in the main grid voltage values and current harmonic frequency range (50Hz-1000Hz corresponding 314rad/sec-6280rad/sec), that the Bode diagram of the two compensations is nearly the same. At opposite, in high frequency range, the differences are obvious.

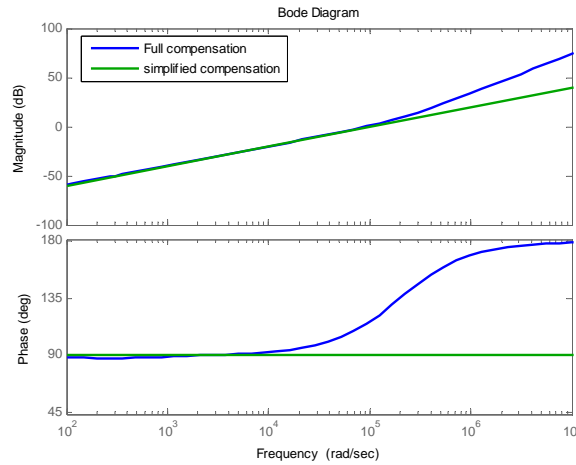


Figure 7. Differences of full compensation and simplified compensation in frequency domain

The derivation element would amplify the noise of grid voltage measurement. By selecting sampling point during one PWM period, the noise can be reduced, especially the switching transient noise.

## 5. Improvements for simplified phase error compensation

By choosing the inverter-side control strategy and phase error compensation based on (11), this section studies influences on the compensation strategies for different electromagnetic environments. As the simplified compensation is performed by differential operation on the grid voltage signal, in strong electromagnetic interference environment, the grid voltage signal noise could be over amplified and thus, worsen the operation. So the simplified phase error compensation cannot be directly implemented. In such case, regeneration of smooth

grid voltage is proposed using PLL. For moderate electromagnetic environment, the simplified compensation could be directly performed, and the use of passive damping resistor could further improve power quality.

**5.1. Fundamental compensation using PLL**

Firstly, for grid connected-system, grid voltage phase is measured by a PLL (cf. Santos Filho *et al.*, 2008), which also outputs the amplitude of fundamental voltage. Using PLL output amplitude and phase, a smooth fundamental voltage can be regenerated. Thus, it can be used for compensation without noise derivation problem. Compared with the real grid voltage signal, the generated signal contains only the fundamental information and the harmonic signals are not involved. So, in this study, using this generated signal is referred to as fundamental compensation.

**5.2. Passive damping**

The capacitor branch includes a serial resistor  $R$  that provides passive damping of resonance effects. The capacitor branch transfer function can be:

$$G_2 = \frac{1}{Cs} + R = \frac{RCs + 1}{Cs} \tag{12}$$

Hence, the compensation transfer function is as in (13), and the compensation control structure is shown in Figure 8a.

$$G_{COMP\_SIMP} = \frac{1}{G_2} = Cs \cdot \frac{1}{RCs + 1} \tag{13}$$

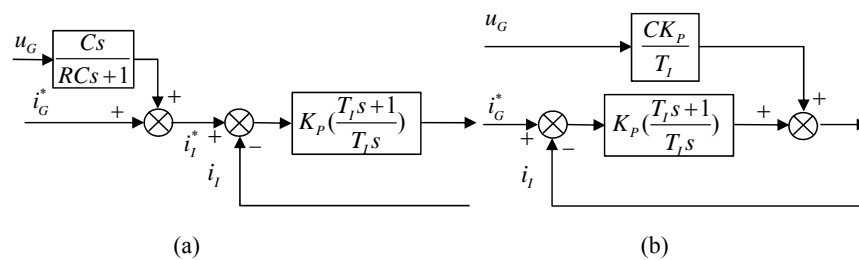


Figure 8. Compensation structure using passive damping by PI controller: (a) compensation control structure, (b) equivalent derived structure

This compensation structure is based on PI controller that is easy for tuning. The PI controller equation is shown in (14).

$$G_{C(PI)} = K_P + \frac{K_I}{s} = K_P \left( \frac{T_I s + 1}{T_I s} \right) \quad \text{with } T_I = \frac{K_P}{K_I} \quad (14)$$

If the PI controller parameter is designed to obtain  $T_I = RC$ , the derivation and filter in compensation transfer function can also be replaced by proportional gain after several transfer function derivation. The final compensation transfer function structure is shown in Figure 8b.

Compared with active damping techniques, the major disadvantage of passive damping is power loss in the damping resistor. The power loss is calculated by (15).

$$P_R = R i_C^2 = \frac{R u_C^2 \omega^2 C^2}{1 + R^2 C^2 \omega^2} \quad (15)$$

where  $\omega = 2\pi f_G$ . By a well parameter selection, the power loss can be negligible compared with the injected power. Neglecting the inductor voltage drop and making the approximation  $u_C \approx u_G$ , the power loss relationship with capacitor vs resistor values can be drawn as shown in Figure 9. The power loss is less than 0.5% of rated injection power, which is 2000W in this study case.

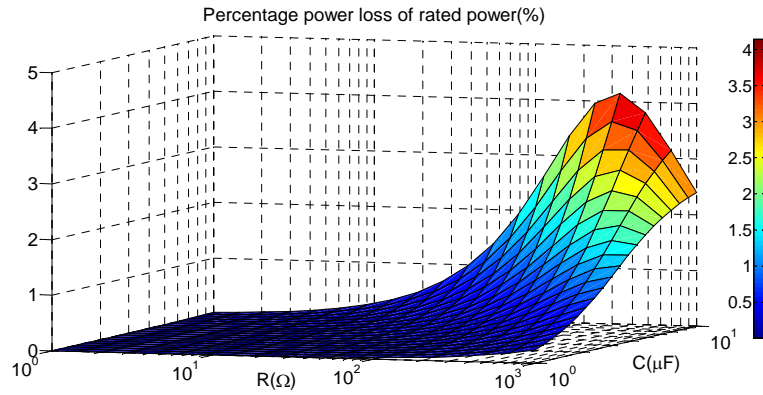


Figure 9. Passive damping power loss relationship with capacitor vs resistor values

## 6. Experimental results

In this section, experimental tests show results concerning phase error for LCL filter control strategy cases: without compensation, fundamental compensation, simplified compensation, as well as simplified compensation with passive damping. In order to compare different control strategies with strictly the same experimental

condition, the solar irradiation based low power PV operation is emulated by constant DC supply with constant voltage at 400V. The experiment platform, used to validate these results, is based on Figure 1. It refers mainly to grid emulator (linear amplifier 3kVA), DC power supply, dSPACE 1103 controller board, and power electronic necessary devices (SEMIKRON SKM100GB063D, 600V-100A). The experimental data are recorded by Fluke 43B power quality analyzer.

The parameters values of LCL filter should be selected according to the following criteria:  $L_f$  should keep low inverter current ripple,  $C$  and  $R$  must be able to give a low damping loss, and  $L_G$  should maintain resonance frequency under control.

Power Factor (PF) and Displacement Power Factor (DPF) are used to describe the phase error and power quality with consideration of both fundamental frequencies and harmonics. For the single phase system, they are defined in (16).

$$PF = \frac{P}{S} = \frac{P}{UI} \quad DPF = \cos \varphi_1 \quad (16)$$

where,  $P$  is the overall active power,  $S$  is the overall apparent power,  $U$  is the root mean square (RMS) value of phase voltage and  $I$  is the phase current RMS value,  $\varphi_1$  is the phase error between fundamental voltage and fundamental current. A large difference between PF and DPF signifies obvious harmonic presence.

The current and voltage total harmonic distortion (THD) are defined as:

$$THD = \frac{\sqrt{\sum_{N=2}^{50} X_N^2}}{X} \quad (17)$$

where  $X_N$  ( $N=2,3,\dots,50$ ) are the corresponding harmonic RMS values of current or voltage,  $X$  is the RMS values of the measured signal.

In the experimental results, the current references are all given at 1A peak in phase with the grid voltage. Figure 10 shows the experimental result of phase error compensation by different control strategy under distorted grid voltage. Due to grid access specific and restrictive conditions, for this experiment, the grid voltage is emulated by linear amplifier with measuring the real grid voltage in real time, which has an average THD of 3%. Figure 10 gives the waveforms and power information of different compensation strategy. The active powers for all cases are around 155W, but large reactive power difference can be seen. Without compensation, the reactive power is 216VAR and the current amplitude is not well controlled with peak value about 2A, as shown in Figure 10a.

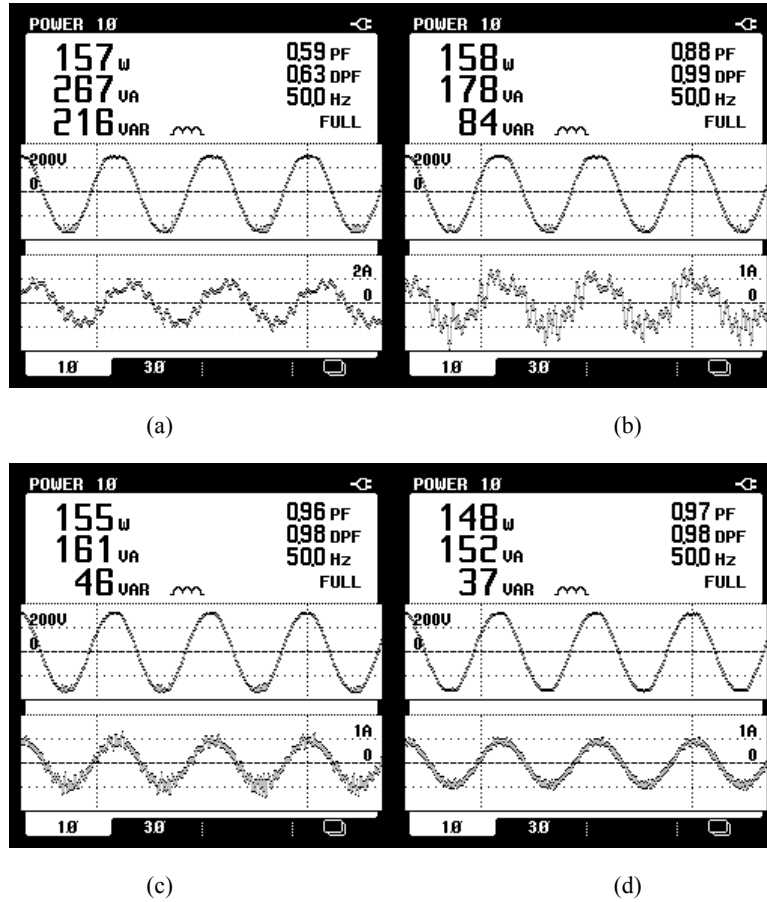


Figure 10. Experimental waveforms with peak current reference 1A following different compensation strategies: (a) no compensation, (b) fundamental compensation, (c) simplified compensation, (d) simplified compensation with passive damping

Compared with no compensation, in cases of fundamental compensation, simplified compensation and simplified compensation with passive damping, the reactive power is reduced by 61.1%, 78.7%, 82.9% respectively, as shown in Figures 10b, 10c, 10d. These results show that any of the compensations could significantly reduce the reactive power introduced by grid voltage. Thus, they can be used to improve the power factor.

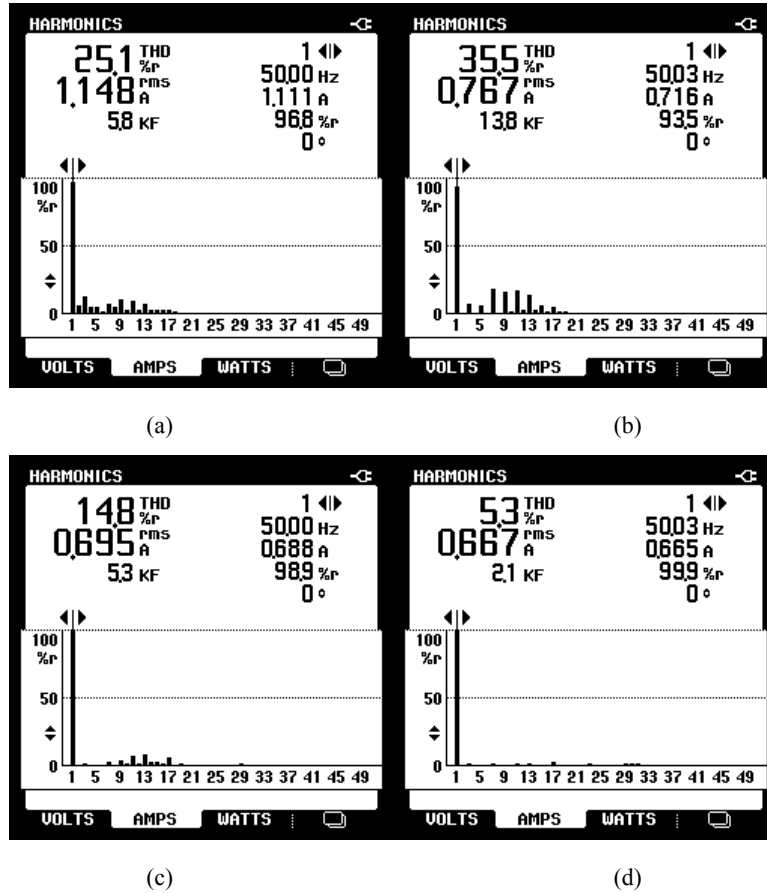


Figure 11. Current distortion in frequency domain with peak current reference 1A following different compensation strategies: (a) no compensation, (b) fundamental compensation, (c) simplified compensation, (d) simplified compensation with passive damping

Figure 11 gives the grid current distortion in frequency domain. In order to compare harmonics for different cases in the same scale, the percentage data are translated in the absolute total harmonic root square value by (18), which is derived from (17).

$$I_H = \sqrt{I_2^2 + I_3^2 + \dots + I_N^2} = THD \cdot I \quad (18)$$

Following (18), for four cases, which are no compensation, fundamental compensation, simplified compensation and simplified compensation with passive damping, the absolute total harmonic mean square value are 0.288A, 0.272A,

0.103A, 0.035A respectively. Compared with no compensation, the total harmonics are reduced by 5.6%, 64.2% and 87.8% for fundamental compensation, simplified compensation and simplified compensation with passive damping respectively. Since the fundamental compensation signal does not contain harmonic information, the harmonic reduction is not obvious.

## 7. Conclusions

For grid-connected PV systems, LCL filter offers high power quality for grid current injection in case of rated power. But the grid voltage introduced reactive power and harmonics exists in the whole power operating range and results in obvious power factor degradations in low power operation, which is inevitable from solar irradiance variation, hence it must be improved. After studying the phase error cause of different control strategies by transfer function, a phase error compensation structure is proposed for inverter-side current feedback structure. Taking into account the no compensation case, three different compensations (fundamental compensation, simplified compensation, and simplified compensation with passive damping) are comparatively studied for different grid-connected situations.

Fundamental compensation is suitable for no distorted grid voltage or in an environment with strong electromagnetic disturbances. Simplified compensation can be used in an environment with less electromagnetic disturbances. The passive damping can be added for further improve power quality at the cost of additional power loss.

The experimental results show that different compensation strategies can significantly reduce the unnecessary reactive power introduced by the grid voltage in low power operation by 61.1%-82.9%. Current harmonics can be reduced by 5.69%-87.8%. The fundamental compensation gives good performance in reactive power rejection, but poor in harmonic reduction; it could be used for situations with strong noise interference where other two compensations do not work well. Simplified compensation gives good performance, but the grid current distortion is the shortage; it is suitable for situations not demanding very high power quality. Simplified compensation with passive damping gives the best performance in power quality; damping power loss could be the shortage, however, by properly selecting the damping resistor and capacitor value, the power loss can be controlled quite reasonably. Simplified compensation with passive damping is suitable for situations where high power quality is given priority.

Concerning a better PV grid-connected system integration, the simplified compensation with passive damping is recommended. It is simple and gives the least harmonic pollution into the grid in low power operations. The reduction of reactive power and harmonics is also suited for the whole operation range and high power quality can be obtained.

## Bibliography

- Abeyasekera T., Johnson C.M., Atkinson D.J. and Armstrong M. (2005). Suppression of line voltage related distortion in current controlled grid connected inverters. *Power Electronics, IEEE Transactions on*, vol. 20, n° 6, p. 1393-1401.
- Agorreta J.L., Borrega M., Lopez J. and Marroyo L. (2011). Modeling and Control of N-Paralleled Grid-Connected Inverters With LCL Filter Coupled Due to Grid Impedance in PV Plants. *Power Electronics, IEEE Transactions on*, vol. 26, n° 3, p. 770-785.
- Dannehl J., Liserre M. and Fuchs F.W. (2011). Filter-Based Active Damping of Voltage Source Converters With LCL Filter. *Industrial Electronics, IEEE Transactions on*, vol. 58, n° 8, p. 3623-3633.
- Dannehl J., Fuchs F.W., Hansen S. and Thogersen P.B. (2010). Investigation of Active Damping Approaches for PI-Based Current Control of Grid-Connected Pulse Width Modulation Converters With LCL Filters. *Industry Applications, IEEE Transactions on*, vol. 46, n° 4, p. 1509-1517.
- Dannehl J., Fuchs F.W. and Thogersen P.B. (2010). PI State Space Current Control of Grid-Connected PWM Converters With LCL Filters. *Power Electronics, IEEE Transactions on*, vol. 25, n° 9, p. 2320-2330.
- Dannehl J., Wessels C. and Fuchs F.W. (2009). Limitations of Voltage-Oriented PI Current Control of Grid-Connected PWM Rectifiers With LCL Filters. *Industrial Electronics, IEEE Transactions on*, vol. 56, n° 2, p. 380-388.
- Fei L., Yan Z., Shanxu D., Jinjun Y., Bangyin L. and Fangrui L. (2009). Parameter Design of a Two-Current-Loop Controller Used in a Grid-Connected Inverter System With LCL Filter. *Industrial Electronics, IEEE Transactions on*, vol. 56, n° 11, p. 4483-4491.
- Figueres E., Garcera G., Sandia J., Gonzalez-Espin F. and Rubio J.C. (2009). Sensitivity Study of the Dynamics of Three-Phase Photovoltaic Inverters With an LCL Grid Filter. *Industrial Electronics, IEEE Transactions on*, vol. 56, n° 3, p. 706-717.
- Gabe I.J., Montagner V.F. and Pinheiro H. (2009). Design and Implementation of a Robust Current Controller for VSI Connected to the Grid Through an LCL Filter. *Power Electronics, IEEE Transactions on*, vol. 24, n° 6, p. 1444-1452.
- Guoqiao S., Xuancai Z., Jun Z. and Dehong X. (2010). A New Feedback Method for PR Current Control of LCL-Filter-Based Grid-Connected Inverter. *Industrial Electronics, IEEE Transactions on*, vol. 57, n° 6, p. 2033-2041.
- Harnefors L., Zhang L. and Bongiorno M. (2008). Frequency-domain passivity-based current controller design. *Power Electronics, IET*, vol. 1, n° 4, p. 455-465.
- Hea-Gwang J., Kyo-Beum L., Sewan C. and Woojin C. (2010). Performance Improvement of LCL-Filter-Based Grid-Connected Inverters Using PQR Power Transformation. *Power Electronics, IEEE Transactions on*, vol. 25, n° 5, p. 1320-1330.
- Houssamo I., Locment F. and Sechilariu M. (2010). Maximum power tracking for photovoltaic power system: Development and experimental comparison of two algorithms. *Renewable Energy*, vol. 35, n° 10, p. 2381-2387.

- Jalili K. and Bernet S. (2009). Design of LCL Filters of Active-Front-End Two-Level Voltage-Source Converters. *Industrial Electronics, IEEE Transactions on*, vol. 56, n° 5, p. 1674-1689.
- Mariethoz S. and Morari M. (2009). Explicit Model-Predictive Control of a PWM Inverter With an LCL Filter. *Industrial Electronics, IEEE Transactions on*, vol. 56, n° 2, p. 389-399.
- Mohamed Y.A.R.I. (2011). Mitigation of Dynamic, Unbalanced, and Harmonic Voltage Disturbances Using Grid-Connected Inverters With LCL Filter. *Industrial Electronics, IEEE Transactions on*, vol. 58, n° 9, p. 3914-3924.
- Santos Filho R.M., Seixas P.F., Cortizo P.C., Torres L.A.B. and Souza A.F. (2008). Comparison of Three Single-Phase PLL Algorithms for UPS Applications. *Industrial Electronics, IEEE Transactions on*, vol. 55, n° 8, p. 2923-2932.
- Sung Yeul P., Chien Liang C., Jih Sheng L. and Seung Ryul M. (2008). Admittance Compensation in Current Loop Control for a Grid-Tie LCL Fuel Cell Inverter. *Power Electronics, IEEE Transactions on*, vol. 23, n° 4, p. 1716-1723.
- Xuehua W., Xinbo R., Shangwei L. and Tse C.K. (2010). Full Feedforward of Grid Voltage for Grid-Connected Inverter With LCL Filter to Suppress Current Distortion Due to Grid Voltage Harmonics. *Power Electronics, IEEE Transactions on*, vol. 25, n° 12, p. 3119-3127.

Received: 12 September 2012

Accepted: 6 September 2013

